AMERICAN JOURNAL OF PHYSIOLOGY
ENDOCRINOLOGY AND METABOLISM

Am J Physiol Endocrinol Metab 328: E311–E324, 2025.
First published January 17, 2025; doi:10.1152/ajpendo.00220.2024

METHODS AND RESOURCES

Proteomic profiling reveals alterations in metabolic and cellular pathways in severe obesity and following metabolic bariatric surgery

Prince Dadson,[1,2]* Miikka-Juhani Honka,[1,2,3]* Tomi Suomi,[4] P. A. Nidhina Haridas,[5] Anne Rokka,[4] Senthil Palani,[1] Elena Goltseva,[6] Ning Wang,[4] Anne Roivainen,[1,7] Paulina Salminen,[7,8,9] Peter James,[4,6] Vesa M. Olkkonen,[5,10] Laura L. Elo,[4,10] and Pirjo Nuutila[1,12]

[1]*Turku PET Centre, University of Turku, Turku, Finland;* [2]*Turku PET Centre, Turku University Hospital, Turku, Finland;* [3]*Division of Information Science, Nara Institute of Science and Technology, Ikoma, Japan;* [4]*Turku Bioscience Centre, University of Turku and Åbo Akademi University, Turku, Finland;* [5]*Minerva Foundation Institute for Medical Research, Helsinki, Finland;* [6]*Department of Immunotechnology, Lund University, Lund, Sweden;* [7]*InFLAMES Research Flagship Center, University of Turku, Turku, Finland;* [8]*Department of Surgery, University of Turku, Turku, Finland;* [9]*Division of Digestive Surgery and Urology, Turku University Hospital, Turku, Finland;* [10]*Department of Anatomy, Faculty of Medicine, University of Helsinki, Helsinki, Finland;* [11]*Institute of Biomedicine, University of Turku, Turku, Finland; and* [12]*Department of Endocrinology, Turku University Hospital, Turku, Finland*

Abstract

In this study, we investigated the impact of bariatric surgery on the adipose proteome to better understand the metabolic and cellular mechanisms underlying weight loss following the procedure. A total of 46 patients with severe obesity were included, with samples collected both before and after bariatric surgery. In addition, 15 healthy individuals without obesity who did not undergo surgery served as controls and were studied once. We utilized quantitative liquid chromatography-tandem mass spectrometry analysis to conduct a large-scale proteomic study on abdominal subcutaneous biopsies obtained from the study participants. Our proteomic profiling revealed that among the 2,254 compared proteins, 46 were upregulated and 34 were downregulated 6 months post surgery compared with baseline [false discovery rate (FDR) < 0.01]. We observed a downregulation of proteins associated with mitochondrial integrity, amino acid catabolism, and lipid metabolism in the patients with severe obesity compared with the controls. Bariatric surgery was associated with an upregulation in pathways related to mitochondrial function, protein synthesis, folding and trafficking, actin cytoskeleton regulation, and DNA binding and repair. These findings emphasize the significant changes in metabolic and cellular pathways following bariatric surgery, highlighting the potential mechanisms underlying the observed health improvements postbariatric surgery. The data provided alongside this paper will serve as a valuable resource for the development of targeted therapeutic strategies for obesity and related metabolic complications. ClinicalTrials.gov registration numbers: NCT00793143 (registered on 19 November 2008) (https://clinicaltrials.gov/ct2/show/NCT00793143) and NCT01373892 (registered on 15 June 2011) (https://clinicaltrials.gov/ct2/show/NCT01373892).

NEW & NOTEWORTHY Our study investigates the effects of metabolic bariatric surgery on adipose tissue proteins, highlighting the mechanisms driving weight loss postsurgery. Through extensive proteomic analysis of adipose biopsies from patients with severe obesity pre- and postsurgery, alongside healthy subjects without obesity, we identified significant alterations in metabolic pathways. These findings provide insights into potential therapeutic targets for obesity-related complications.

adipose tissue; metabolic and cellular pathways; metabolic bariatric surgery; proteomics; severe obesity

INTRODUCTION

Obesity, a multifactorial disease and growing global health concern, is associated with a range of metabolic and cellular alterations that fundamentally disrupt physiological and metabolic processes in the body (1). Characterized by an excessive accumulation of adipose tissue, obesity contributes to the development of chronic diseases, including type 2 diabetes mellitus (T2DM), cardiovascular disorders, and a host of associated complications (2).

Adipose tissue plays pivotal roles in systemic energy homeostasis, lipid metabolism, and insulin-responsive glucose metabolism (3, 4). During obesity, expansion of abdominal subcutaneous adipose tissue (SAT) is characterized by adipocyte hyperplasia and hypertrophy, which result in increased adipocyte hypoxia, adipocyte cell death, recruitment of pro-

*P. Dadson and M.-J. Honka contributed equally to this work.
Correspondence: P. Nuutila (pirjo.nuutila@utu.fi).
Submitted 10 June 2024 / Revised 12 July 2024 / Accepted 17 December 2024

inflammatory cells, impairment of energy (e.g., glucose and lipid) metabolism (5), insulin resistance, and T2DM (6, 7). Further investigations are needed to explore the molecular and cellular mechanisms contributing to the expansion of abdominal adipose tissue and their role in the impaired energy metabolism in persons with obesity.

Mitochondria are involved in a wide range of fundamental cellular processes and are central to energy metabolism, including oxidative phosphorylation (8), fatty acid oxidation, thermogenesis, and branched-chain amino acid (BCAA) catabolism (9, 10). In obesity, mitochondrial dysfunction within adipose tissue leads to energy dysregulation, typically resulting in increased production of reactive oxygen species (ROS) contributing to oxidative stress, inflammation, insulin resistance, and the disruption of metabolic homeostasis (11). Although it is known that mitochondrial dysfunction plays a role in obesity, the exact underlying mechanisms are still under investigation.

Bariatric surgery is recognized as the most effective treatment for achieving sustained weight loss in individuals suffering from severe obesity complicated by comorbidities such as T2DM and other cardiometabolic abnormalities (12). This procedure significantly improves adipose tissue metabolic function and whole-body insulin sensitivity, and results in diabetes remission (13, 14). However, the underlying mechanisms of these improvements have not yet been fully understood. In this study, we utilize liquid chromatography-tandem mass spectrometry (LC-MS/MS) for a large-scale quantification of adipose tissue-specific proteins associated with metabolic and cellular alterations in the context of severe obesity and their response to bariatric surgery-induced weight loss. We anticipate that the functional characterization of proteins in adipose tissue may contribute to our understanding of the pathophysiology of inflammation, insulin resistance, T2DM, and excess abdominal fat in persons with obesity and may also offer novel targets for therapeutic interventions for individuals with obesity-related T2DM complications. For this purpose, we have deposited the mass spectrometry proteomics data to a public database and shared the complete results of differential protein expression and gene set enrichment analyses as supplements to this paper.

MATERIALS AND METHODS

Human Participants

Datasets from two bariatric surgery positron emission tomography studies were combined for the current study (Fig. 1). A total of 52 participants (5 men and 47 women) with severe obesity were recruited from individuals undergoing bariatric surgery at the Hospital District of Southwest Finland. Inclusion criteria included an age range of 18–60 yr and body mass index (BMI) of $\geq$ 40 kg/m^2 (or $\geq$35 kg/m^2 with an additional obesity-related comorbidity). Fifteen age-matched metabolically healthy volunteers served as controls. The protocols were approved by the Ethics Committee of the Wellbeing Services County of Southwest Finland and were conducted in compliance with the Code of Ethics of the World Medical Association (Helsinki Declaration). The characteristics of the human participants can be found in Supplemental Table S1 (15). All the participants provided written informed consent.

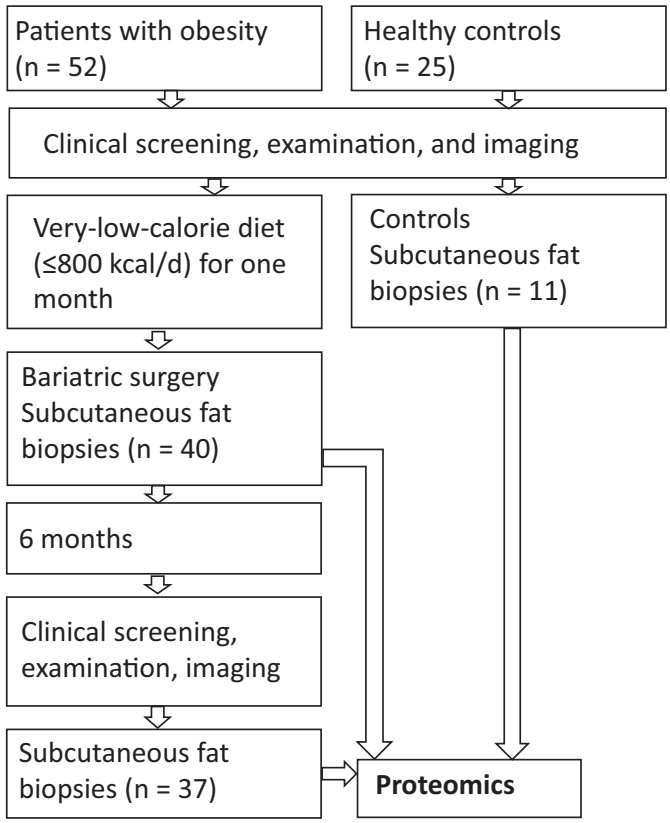

Figure 1. Participants' flow diagram.

Study Design

This study recruited individuals with severe obesity and screened them for medical history, conducted physical examinations, obtained anthropometric measurements, carried out blood tests, and performed oral glucose tolerance tests, as previously described (16) (Fig. 1). The person with severe obesity followed a 4-wk very-low-calorie diet (800 kcal/day) before undergoing metabolic bariatric surgery. Among them, 22 participants underwent sleeve gastrectomy and 27 underwent Roux-en-Y gastric bypass surgery. Postbariatric surgery studies were conducted 6 mo after the surgical intervention. Of the 49 participants who underwent surgery, 3 withdrew from the postoperative studies for personal reasons (Fig. 1). Among the 46 participants with severe obesity, 18 had T2DM and out of the 28 participants without T2DM, 11 had impaired fasting glucose or impaired glucose tolerance (16).

Biochemical and immunological analyses.

Plasma glucose, glycated hemoglobin, serum insulin, and high-sensitivity C-reactive protein were measured as previously described (16). Glycemic indices, including a standard 75 g oral glucose tolerance test and homeostasis model assessment of insulin resistance defined as (Glucose 0 min $\times$ Insulin 0 min)/22.5 (17), were assessed. Stored serum samples were analyzed for cytokine and adipokine levels using the Bio-Plex 200 system (Bio-Rad Laboratories, Inc., California) together

with Bio-Plex Manager Software version 4.1. Multiplex quantification of cytokines was performed using the MILLIPLEX MAP Kit Human Adipokine Magnetic Bead Panels 1 and 2 (Millipore Corporation, Massachusetts).

Body composition measurement.

Body fat content was measured using bioimpedance with an electrical scale (Omron BF400). Abdominal SAT volumes were assessed using magnetic resonance imaging (Philips Medical Systems, Best, The Netherlands), as previously described (18, 19).

Indirect calorimetry.

Open-system indirect calorimetry (Deltatrac) was used to quantify O_2 consumption ($\dot{V}O_2$) and CO_2 production ($\dot{V}CO_2$), from which whole-body energy expenditure and lipid and fat oxidation rates were calculated as previously described (20). The resting energy expenditure (REE) was calculated as REE (kcal/day) = $(3.941 \times \dot{V}CO_2 + 1.11 \times \dot{V}O_2) \times 1.44$ (21).

Tissue Biopsy Collection

Biopsies from SAT were collected during bariatric surgery and 6 mo postoperatively under local anesthesia using 1% lidocaine without adrenaline. In addition, SAT biopsies from healthy controls without obesity were collected for reference. The biopsies were obtained by a surgical excision. The size of the original fat biopsies was 150–1,000 mg which was cut into smaller pieces. The samples collected were stored in two different ways: samples used for immunohistochemistry were stored in 10% formalin, whereas samples used for proteomics (at minimum a 50-mg piece) were frozen in liquid nitrogen and stored at −70°C. The minimum sample amount of 50 mg was determined to yield a sufficient amount of protein based on a preliminary analysis of adipose tissue test samples before commencing the actual study.

Adipocyte cell size measurements.

Hematoxylin-eosin-stained slides from the SAT biopsies were digitally scanned with the Pannoramic slide scanner system (v1.15.4; 3DHISTECH, Budapest, Hungary). The mean adipocyte size values were measured following the previously described methodology (18, 22).

Proteomics

Sample preparation.

The SAT biopsy samples from individuals with severe obesity, both before ($n = 40$) and after ($n = 37$) bariatric surgery, as well as from the control group ($n = 11$), were utilized for the sample preparation and subsequent proteomic analysis. To prepare the samples, 500 μL of lysis buffer containing 1% sodium deoxycholate in 50 mM Tris-HCl (pH 8) with complete ethylenediaminetetraacetic acid-free protease inhibitor cocktail (Merck) was added to frozen adipose samples (∼100 mg), which were then homogenized with a TissueLyser LT instrument (QIAGEN) at +4°C, with two 60 s cycles at 50 Hz and intermittent 5 min cooling on ice. Samples were incubated on ice for 30 min and then centrifuged for 5 min at 16,000 *g* at 4°C. The protein fraction was collected from underneath a lipid layer and transferred to a new Eppendorf tube. Protein concentrations were determined using a NanoDrop device (Thermo Scientific) by measuring absorbance at 280 nm. To remove some of the blood proteins present in the adipose samples, the depletion of 12 high-abundant serum proteins was performed by Top12 Abundant Protein Depletion Spin Columns (Pierce Thermo, no. 85165) according to the manufacturer's protocol. For the depletion, 250 μg of total protein was taken. Samples were concentrated using 10 kDa cut-off centrifugal filters (Microcon, MRCPRT010) before and after depletion to reduce the sample volume. Protein concentrations of the depleted samples were measured with BioRad's Bradford protein assay. When possible, 50 μg of each depleted sample was used for in-solution digestion. Proteins were reduced with dithiothreitol, then alkylated with iodoacetamide, and digested with trypsin at a trypsin:protein ratio of 1:25. Sodium deoxycholate was removed before desalting by briefly acidifying the digested samples and centrifugation at 16,000 *g* for 20 min. Desalting was performed with 96-well C18 plate (Waters) according to the manufacturer's standard protocol. Peptides were eluted with 0.1% formic acid in 50% acetonitrile. Before LC-MS/MS analysis, peptides were dissolved in 0.1% formic acid and 500 ng of each sample was analyzed based on the previously determined protein concentrations.

LC-MS/MS analysis.

The LC-MS/MS analyses were performed on a nanoflow high-performance liquid chromatography (HPLC) system (Easy-nLC1200, Thermo Fisher Scientific) coupled to a Q Exactive HF mass spectrometer (Thermo Fisher Scientific, Bremen, Germany) equipped with a nanoelectrospray ionization source. Peptides were first loaded on a 2-cm trapping column and subsequently separated inline on a 15-cm C18 column (75 μm × 15 cm, ReproSil-Pur 5 μm 200 Å C18-AQ, Dr. Maisch HPLC GmbH, Ammerbuch-Entringen, Germany). The mobile phase consisted of water with 0.1% formic acid (*solvent A*) or acetonitrile/water [80:20 (vol/vol)] with 0.1% formic acid (*solvent B*). A 120-min chromatographic method was used to elute peptides (90-min gradient from 6% to 35% *solvent B*, following 8 min from 35% to 100% *solvent B*) followed by reequilibration with A. The flow rate was 300 nL/min. MS data were acquired automatically using Thermo Xcalibur 4.1 software (Thermo Fisher Scientific). A data-dependent acquisition method consisted of an Orbitrap MS survey scan of mass range 300–2,000 m/z followed by higher-energy collisional dissociation (HCD) fragmentation of the 10 most intense peptide ions in each scan cycle.

The raw MS files were processed with MaxQuant (version 1.6.5.0) (23). The spectra were searched against a UniProt/Swiss-Prot Homo sapiens database (4 May 2019, 20,418 entries). Matching between runs was used, with a matching time window of 0.7 min and an alignment time window of 20 min. Methionine oxidation and N-terminal acetylation were defined as variable modifications, and cysteine carbamidomethylation was defined as a fixed modification. Trypsin was selected for protein digestion allowing up to two miscleavages. The false discovery rate (FDR) was set to 1% for both peptide and protein identifications. Protein quantification is based on the sum of all identified peptide-ion intensities (MS).

Quantification and Statistical Analysis

The R environment (v. 4.0.4) was used for data analysis. Identifications to reverse peptide sequences and known contaminants were filtered from the data, and only proteins identified by two unique peptides were kept. This leaves 2,752 individual proteins or sets of indistinguishable proteins identified from the SAT specimens. Proteins with an overall estimated intensity of zero were replaced by NA to denote missing values. None of the detected proteins were completely missing in any of the presurgery, postsurgery, or control groups, and only a few proteins had a high proportion of missingness (>66% missing) in at least one of the study groups as illustrated in the Supplemental Fig. S1 (15). The intensity matrix of all samples was normalized using variance stabilization normalization (24). To filter adipose tissue samples that were contaminated with blood, a specialized scoring metric was used. Signature lists were acquired from the Human Protein Atlas (25) for adipose tissue (168 elevated proteins) and from the Human Blood Atlas for blood (26) (207 elevated proteins). Calculating the score for each sample was done by first calculating the difference of protein intensities to their mean value over all samples, then performing a ranked gene set enrichment analysis (27) against the signature sets. The final score for each of the samples was defined as:

$$\text{score} = \frac{[(1 - P_{\text{adipose}}) \times \text{sign}(\text{ES}_{\text{adipose}})] - [(1 - P_{\text{blood}}) \times \text{sign}(\text{ES}_{\text{blood}})]}{2}$$

where ES is the enrichment score, and P is its significance. The final score ranging from 1 (adipose tissue) to −1 (blood) represents the estimated bias. A total of 13 samples with the highest blood-like signature were removed before further analysis (including SAT bariatric surgery 7, after surgery 4, controls 2) based on them being below the selected cutoff of −0.75.

Differential expression between samples from bariatric surgery and after surgery was compared using linear mixed effects model, where the potential confounding from weight at surgery, weight loss during presurgery very low-calorie diet, surgery type, diabetes status, as well as lipid, blood pressure, and diabetes medication was accounted for. In addition, sex and each individual were considered as random terms in the model. We used a filtering criterion of having at least 50% of non-missing values over all the samples when comparing the samples from bariatric surgery and after surgery to ensure that there were sufficient number of cases to have representative samples for the covariates used in the linear mixed effects models. Comparisons between the bariatric surgery and after surgery samples versus controls without obesity were performed using the Reproducibility-Optimized Test Statistic (R package ROTS) (28), which has been shown to have excellent performance for the statistical analysis of differential protein expression data in several benchmarking studies (29–31). In the ROTS analyses, each of the tested groups had at least three nonmissing values for each comparison. The number of bootstrap samples (B) was set to 1,000, and the largest top-list size to be considered (K) was set as the size of the full data. A paired test was used in comparisons involving measurements before and after surgery from the same individuals. A ranked gene set enrichment analysis for the differential expression results was performed against Molecular Signatures Database (MSigDB, version 2022.1.Hs) using the R package fgsea (32). Spearman's rank correlation was used to estimate the relationships between clinical variables and protein abundances. It was calculated only if there were at least 10 measurements to compare. The heatmaps were drawn using the ComplexHeatmap (33) R package. The protein comparisons and gene set enrichment analyses were adjusted for FDR using the Benjamini–Hochberg method (34). An FDR threshold of 0.01 was used to limit the proportion of false discoveries among the results presented and to focus on the protein findings that are most likely important. The complete results of the differential expression analysis and gene set enrichment analysis are provided as supplemental resources to this paper (15).

RESULTS

The patients who underwent surgery lost an average of 24.5% of their body weight between baseline measurements and 6 mo after surgery [Supplemental Table S1 (15)]. Of the patients with T2DM, 63% experienced remission after surgery. Six months post surgery, an upregulation of 46 proteins and a downregulation of 34 proteins out of the 2,254 compared proteins were observed in SAT (FDR < 0.01) compared with baseline [Supplemental File S1*A* (15)]. The effects of potential confounders such as weight at the time of surgery, weight loss during the presurgery very low-calorie diet, surgery type, diabetes status, as well as lipid, blood pressure, and diabetes medications on these findings were insignificant (Fig. 2). A principal component analysis (PCA) of the proteomics results showed considerable overlap between the postsurgery results and the healthy controls (Fig. 3). In a ranked gene set enrichment analysis, three upregulated and eight downregulated Hallmark gene sets were found when comparing SAT from 6 mo after surgery to the before surgery specimens, reflecting a reversal in several pathways that were dysregulated in the before surgery biopsies (Fig. 4).

Protein expression in SAT was compared between the patients and controls for reference [detailed results are provided in Supplemental File S1, *B* and *C* (15)]. After adjusting for FDR, 25 out of 2,523 proteins were significantly downregulated and 11 proteins were upregulated in SAT of persons with severe obesity presurgery compared with controls [FDR < 0.01; Supplemental File S1*B* (15)]. After surgery, only three SAT proteins were significantly different compared with controls which is in line with the PCA result [Supplemental File S1*C* (15)].

Differential Protein Expression Profiles Highlight Metabolic and Cellular Alterations in Persons with Severe Obesity

In the group with severe obesity (before surgery), a significant decrease in key proteins involved in relevant metabolic pathways was observed when compared with the control group [Supplemental File S1*B* (15)]. Specifically, proteins involved in maintaining a number of fundamental cellular processes, including the integrity of the mitochondrial matrix and RNA localization within cells, were found to be downregulated

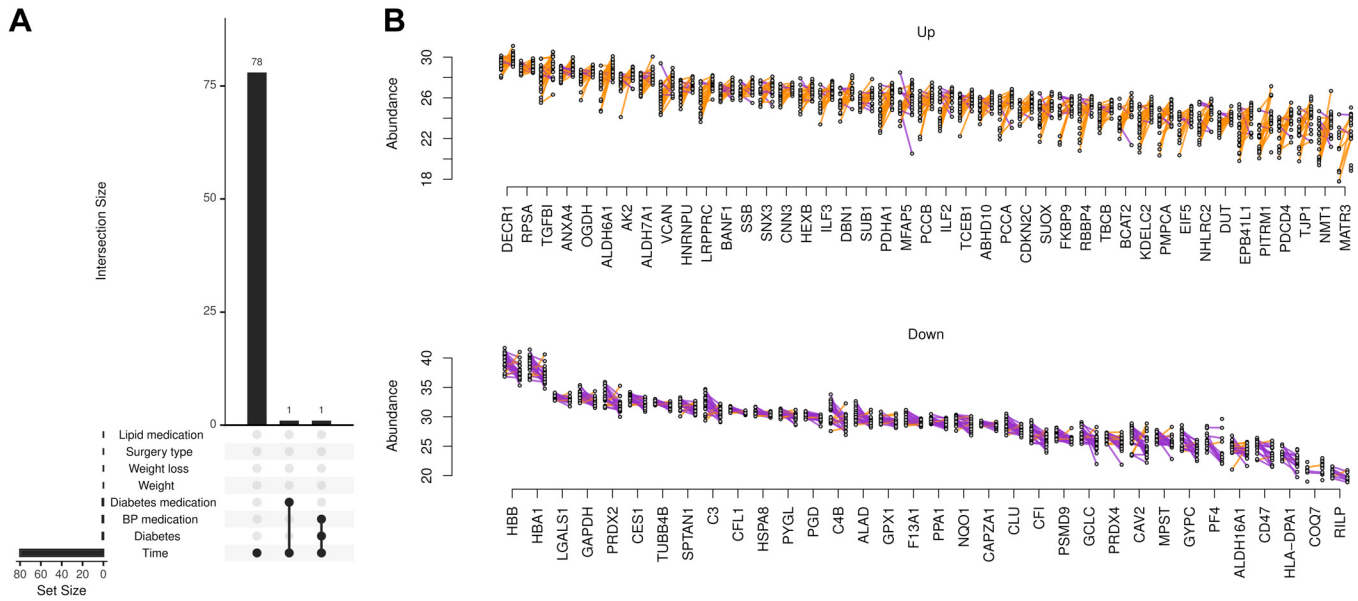

Figure 2. *A*: number of proteins affected by time (post- vs. presurgery), lipid, diabetes, and blood pressure medications, surgery type, weight loss (by presurgery diet), weight, and diabetes based on linear mixed effects analysis. This analysis shows that only two proteins were affected by other factors than time. *B*: change in protein abundance from pre- to postsurgery. All FDR < 0.01. FDR, false discovery rate.

[Supplemental File S2*A* (15)], such as LRPPRC important for maintaining the integrity of the mitochondrial matrix, and COQ9 which is required for the biosynthesis of coenzyme Q10, a vital component of the electron transport chain in mitochondria. In addition, enzymes like ALDH6A1 and BCAT2, which play pivotal roles in cellular amino acid catabolism and BCAA metabolic pathways, were downregulated. Regulatory proteins, including CDKN2C, involved in the regulation of cellular amide metabolic processes and RNA localization, were reduced. Furthermore, enzymes like ACADL, ECHS1, ACADM, and DECR1 were downregulated, which are fundamental to lipid metabolism pathways such as lipid oxidation, lipid modification, fatty acid β-oxidation, and fatty acid catabolic processes. In addition, Hallmark and Gene ontology gene set enrichment analyses were consistent with a decrease in oxidative phosphorylation, fatty acid metabolism, adipogenesis, and cholesterol homeostasis in severe obesity [Fig. 4; Supplemental File S2*A* (15)].

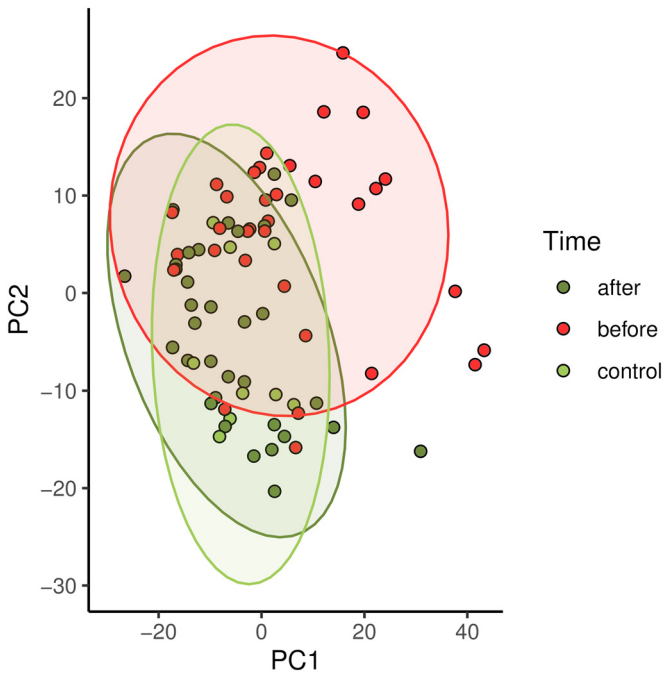

Figure 3. Principal component analysis on the proteome from before and after surgery and from controls. The plot describes how the results from different cases and time points overlap across the two most important principal components. The *principal components 1* and *2* explained 27% and 15% of variance over the protein measurements, respectively.

Proteins associated with cytoskeletal components, cellular organization, and intercellular communication, such as TUBB4B, VIM, PYGL, PPA1, and PSMD14, showed higher expression levels in the group with obesity compared with the controls [Supplemental Files S1*B* and S2*A* (15)]. Moreover, the enrichment analysis indicated an increase in heme metabolism, IL6 JAK STAT3 signaling, KRAS signaling, complement, and coagulation factors in the patients with severe obesity compared with controls (Fig. 4).

Downregulation of Immune, Metabolic, and Structural Proteins following Bariatric Surgery-Induced Weight Loss

Surgery-induced weight loss caused reductions in several pathways that were either significantly or nominally upregulated in individuals with severe obesity before surgery [Fig. 4; Supplemental File S2*B* (15)]. These pathways include the ROS pathway, heme metabolism, complement, coagulation, mTORC1, interferon α and γ responses, as well as KRAS signaling. Moreover, downregulation of several proteins associated with key biological functions was observed postsurgery compared with baseline [Figs. 2 and 5; Supplemental Files S1*A* and S2*B* (15)]. In the category of the complement system and immunity, the downregulation of C4B, C3, CFI, and CD47 may signify adjustments in immune function and

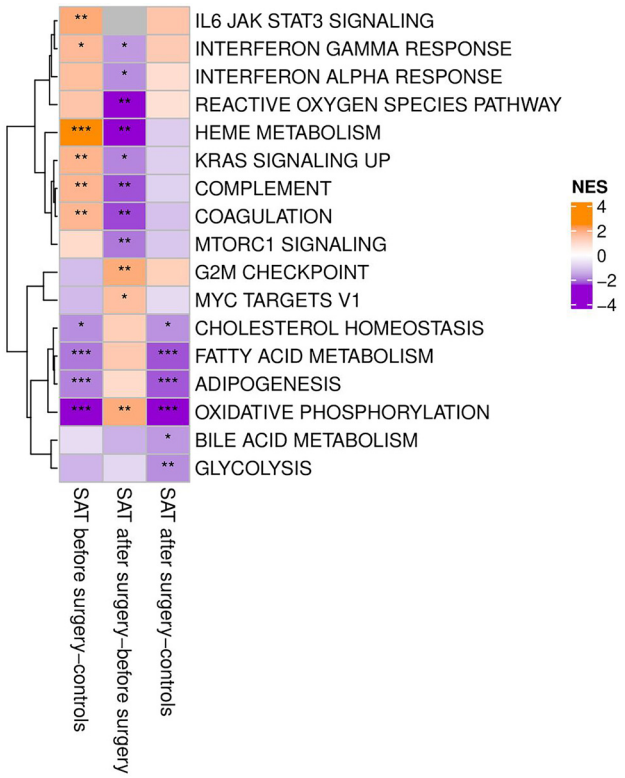

Figure 4. Difference in proteins of the Molecular Signatures Database Hallmark gene sets in subcutaneous adipose tissue when comparing samples taken from patients with severe obesity before or after surgery or from controls without obesity (comparisons explained on the *x*-axis labels). Only proteins that have a significant difference in at least one of the comparisons are shown on the heatmaps. ***adj. $P < 0.001$, **adj. $P < 0.01$, *adj. $P < 0.05$. NES, normalized enrichment score; SAT, subcutaneous adipose tissue.

complement activation postsurgery. Proteins involved in response to oxidative stress and redox balance, as well as detoxification-related genes such as PRDX2, PRDX4, GPX1, and NQO1, were downregulated. In addition, metabolic, and enzyme-related proteins like GCLC, CES1, ALAD, MPST, PGD, PPA1, ALDH16A1, and GCLC, showed decreased expression. Moreover, proteins associated with cellular structure and transport (CAV2, RILP, SPTAN1, and TUBB4B), cellular signaling and transport (CAPZA1, CFL1, CLU, LGALS1, PYGL, and COQ7), as well as proteasome and cellular regulation (PSMD9) were downregulated. The expression levels of proteins involved in pathways of mRNA metabolism and oxidative stress such as G3BP2, and in maintaining cellular energy homeostasis such as CKM, were lower in the patients after surgery compared with controls [Supplemental File S1*C* (15)]. On the contrary, these was little evidence for a difference in mRNA metabolism or oxidative stress pathways in the GSEA analysis after surgery compared with controls, suggesting that these pathways were largely normalized [Supplemental File S2*C* (15)].

Bariatric Surgery Upregulates Metabolic Enzymes and Proteins Involved in a Number of Key Cellular Pathways

Bariatric surgery-induced weight loss increased the expression of oxidative phosphorylation, G2M checkpoint, and MYC targets V1 pathways (Fig. 4). Furthermore, proteins associated with metabolic shifts and an enhanced capacity for protein synthesis, such as RPSA, AK2, and OGDH, showed increased expression [Supplemental Files S1*A* and S2*B* (15)]. Transcription and RNA processing are likely to be influenced by the upregulation of proteins like TCEB1 and various heterogeneous nuclear ribonucleoproteins (HNRNPU, HNRNPCL4, HNRNPCL1, HNRNPCL3, and HNRNPCL2) [Supplemental File S2*B* (15)]. Proteins involved in maintaining cellular structural components and junctional integrity, including CNN3 and TJP1, showed increased expression levels [Supplemental File S1*A* (15)]. In addition, the upregulation of proteins like SSB, ANXA4, and HMGB1 indicated an improved capacity for DNA binding, repair, and genomic stability [Supplemental File S2*B* (15)]. Moreover, proteins like CDKN2C regulating the cell cycle, and EIF5 involved in translation initiation, were upregulated, suggesting enhanced cellular proliferation and protein synthesis. Mitochondrial function is most likely significantly impacted by the upregulation of proteins such as CHCHD2, SUOX, PCCB, PCCA, LRPPRC, and PITRM1 [Supplemental File S2*B* (15)]. Furthermore, a group of proteins associated with the remodeling of the extracellular matrix, including VCAN, TGFBI, and EPB41L1, displayed increased expression after surgery compared with baseline [Supplemental Files S1*A* and S2*B* (15)]. Proteins involved in protein folding and trafficking, such as FKBP9, were upregulated, indicating enhanced protein processing. The upregulation of DBN1 suggested altered regulation of the actin cytoskeleton, contributing to cellular structural changes. Furthermore, the upregulation of NMT1 is suggestive of increased post-translational modification through myristoylation. The expression levels of proteins responsible for tubulin-specific chaperone activity, such as tubulin-specific chaperone D (TBCD), were higher in the postsurgery group with severe obesity compared with controls [Supplemental File S1*C* (15)]. Despite the surgery-induced weight loss, the metabolic processes associated with cholesterol homeostasis, fatty acid metabolism, adipogenesis, oxidative phosphorylation, bile acid metabolism, and glycolysis did not attain a complete return to the normal state in the postsurgery group with severe obesity compared with the controls [Fig. 4; Supplemental File S2*C* (15)].

DISCUSSION

In the present study, we observed significant alterations in the adipose protein expression profiles of individuals with severe obesity both before and after bariatric surgery. Pre surgery, there was a decrease in proteins involved in essential metabolic pathways as compared with healthy controls, contrary to the increased expression of proteins associated with cytoskeletal components, cellular organization, heme metabolism, interferon response, complement, and coagulation. Bariatric surgery induced a profound change in the molecular profile, marked by increases in proteins related to RNA processing, cellular respiration and signaling, as well as decreases in proteins associated with cellular adhesion and lysosomal functions. Importantly, there was an upregulation of metabolic enzymes postsurgery and reductions in heme metabolism, interferon response, complement, and coagulation pathways. Linear mixed effects analysis accounting for possible confounders further confirmed these observed protein expression patterns, emphasizing the significance of the

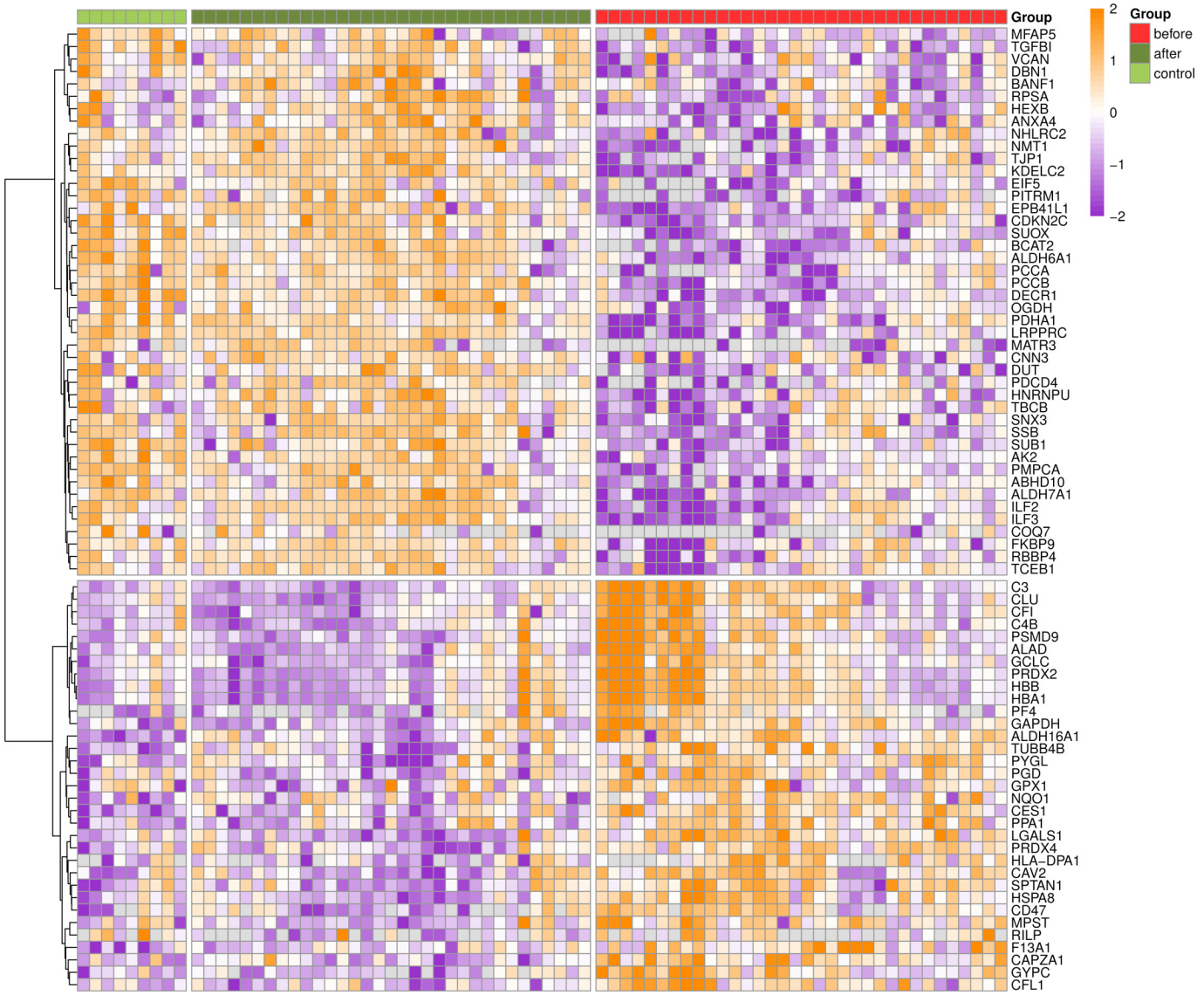

Figure 5. A heatmap describing individual differences in protein abundance across the proteins that were differentially expressed in subcutaneous adipose tissue before and after surgery at group level.

findings. In fact, there was little difference in individual protein abundances when comparing postsurgery results to controls. This may seem surprising when the average BMI of the patients was still above 30 kg/m^2 post surgery. However, we have previously shown that SAT glucose and fatty acid uptake per kg of tissue, SAT adipocyte size as well as fasting insulin and free fatty acid levels were similar or close to those of controls after surgery which aligns with the proteomics findings [Supplemental Table S1 (15, 18, 19)]. On the contrary, results from the enrichment analyses showed that even though differences in the expression of individual proteins between the patients after surgery and controls were minor, on a pathway level, SAT from the patients still showed downregulation of substrate oxidation pathways. In addition, the larger fat mass capable of releasing more fatty acids at fasting state and the fact that the patients were still losing weight probably explains why the patients post surgery had still elevated fatty acid oxidation rates and higher triglycerides compared with controls [Supplemental Table S1 (15, 18, 35)]. Collectively, these results increase our understanding and provide a valuable resource regarding the molecular changes associated with severe obesity, and the impact of weight loss induced by bariatric surgery.

Regulation Mitochondrial Function and Oxidative Phosphorylation Pathway

One of our key findings is the downregulation of proteins vital for maintaining mitochondrial integrity and function, including Leucine-rich PPR motif-containing protein (LRPPRC) and COQ9, in the adipose tissue of individuals with obesity. LRPPRC protects mitochondrial mRNAs from 3′ exoribonuclease digestion and is thus important for maintaining the integrity of the mitochondrial matrix (36). Its reduction causes a reduction of several electron transport chain proteins in the liver, skeletal muscle, and brown adipose tissue which may lead to oxidative dysfunction (37, 38). Thus, the reduced LRPPRC expression may be in part

responsible for the reduction of mitochondrial proteins in obesity. Mitochondrial function was significantly impacted after surgery as indicated by the upregulation of the oxidative phosphorylation pathway and proteins such as SUOX, PCCB, PCCA, LRPPRC, and PITRM1. Increased SAT expression of transcripts related to oxidative phosphorylation has been shown after weight loss induced by bariatric surgery, consistent with the present observations (39). Propionyl-CoA carboxylase (PCC) is the enzyme which catalyzes the carboxylation of propionyl-CoA to methylmalonyl-CoA and is encoded by the genes PCCA and PCCB (40). Coenzyme Q9 homolog (COQ9), on the contrary, is essential for the biosynthesis of coenzyme Q10, a critical component of the electron transport chain in mitochondria. Adipose tissues from patients and mice with insulin resistance show decreased levels of the COQ biosynthetic proteins COQ7 and COQ9, leading to reduced CoQ levels in the mitochondria (41). Furthermore, research has linked lower levels of COQ with higher levels of oxidants in the mitochondria (41).

Modulation of Oxidative Stress, Inflammatory Pathways, and Immune Responses

Increased levels of oxidants often lead to oxidative stress, mitochondrial dysfunction, and increased activation of inflammatory pathways. The downregulation of the ROS pathway and specifically proteins related to oxidative stress response (PRDX2, PRDX4, GPX1, MPST, and NQO1) indicates a potential reduction in oxidative stress and restoration of the redox balance postsurgery. Glutathione peroxidase 1 (GPX1) is a selenium-dependent enzyme that reduces intracellular hydrogen peroxide and lipid peroxides. Global GPX1 deficiency has been reported to enhance insulin sensitivity in mice fed a high-fat/high-sucrose diet (42). In obesity, the generation of ROS exceeds the antioxidant reserve and can contribute to insulin resistance. 3-Mercaptopyruvate sulfurtransferase (MPST) is a redox-sensitive enzyme that belongs to the rhodanese phosphatase superfamily (43). MPST is expressed in adipocytes (44) and is downregulated in obesity (43). Lack of MPST reduces mitochondrial protein import, leading to attenuated β-oxidation, tricarboxylic acid (TCA) cycle, and oxidative phosphorylation, thus increasing lipid storage (43). A partial knockdown of MPST in adipocytes impairs the expression of proteins related to the maintenance of adipocyte function and promotes inflammation (45). Thus, the observed downregulation of MPST post surgery may reflect its reduced need as the adipose tissue metabolic status approaches normal. NQO1 [NAD(P)H Quinone Dehydrogenase 1] plays a direct role in protection from oxidative stress via its activity as a superoxide scavenger (46). NQO1 was found to be highly expressed in both human omental and SAT adipocytes and was positively correlated with BMI, fasting insulin, as well as with the levels of insulin and glucose during oral glucose tolerance test (OGTT) (47). Pharmacological stimulation of NADH oxidation via NQO1-mediated catalysis has been associated with amelioration of both obesity (48) and hypertension (49) in mice, suggesting that NQO1 upregulation may be an effective therapeutic strategy for treating metabolic syndrome. As for MPST, the downregulation of NQO1 post surgery may reflect its reduced need as the adipose tissue metabolic status approaches normal.

The downregulation of inflammatory response, interferon, complement, and coagulation pathways and proteins such as PF4, CD47, HLA-DPA1, and C4B suggests a reduced immune response and inflammation postsurgery compared with baseline. In addition to promoting innate immune responses, platelet factor 4 (PF4) can also inhibit angiogenesis (50). The transmembrane protein CD47 plays a significant role in immune cell communication and cell signaling. CD47 differentially regulates adipose tissue function, contributes to diet-induced obesity, and is associated with its comorbidities (51). CD47-deficient mice were reported to display reduced fasting blood glucose levels, improved glucose tolerance (52), and increased energy expenditure (53). The reduced expression may underly the postbariatric surgery benefits of such improvements in adipose metabolism (19), glycemic, and lipid parameters (18, 19). Major histocompatibility complex, class II, DP α 1 (HLA-DPA1) plays a central role in the immune system by presenting peptides derived from extracellular proteins. Obesity is associated with increased MHC class II antigen presentation in adipocytes, which leads to increased pro-inflammatory T cell activity in adipose tissue (54) and decreased insulin sensitivity (55). C4B contributes to homeostasis by complementing immunological and inflammatory processes (56). Increased serum complement levels are a risk factor for the development of diabetes and a determinant of cardiometabolic risk in adults (57), and increased levels of both C3 and C4 are consistent with an enhanced inflammatory status. Downregulation of proteins related to proteasomal activity (PSMD9 and F13A1) after surgery suggests potential alterations in protein turnover and degradation processes. PSMD9 is a ubiquitous protein contributing to intracellular protein degradation into antigenic peptides during the immune response. It may thus play a role in inflammation as part of autoimmune processes (10). Genetic variants in a locus containing *PSMD9* may contribute to T2DM as well as to obesity, overweight status, and visceral obesity (58). Higher expressions of proteins like PYGL and PPA1 were found in the individuals with obesity compared with controls. The increased PYGL (glycogen phosphorylase L) expression may be related to abnormal adipocyte glycogen accumulation observed in hypoxic and inflamed adipose tissue (59).

Regulation of Adipocyte Function and Cellular Pathways

Cyclin-dependent kinase inhibitor 2 C (CDKN2C, also known as p18) was significantly suppressed in obesity. CDKN2C acts as an important controller of adipocyte differentiation, lipolysis, lipogenesis, and glucose metabolism by exerting an inhibitory effect on cyclin-dependent kinases 4 and 6 (60, 61). CDKN2C plays an important role in adipocyte differentiation and has a distinctively sex-specific expression pattern with higher levels in women (61). In a previous study (62), *CDKN2C* knockdown in preadipocytes led to reduced lipid accumulation during adipocyte differentiation, suggesting that CDKN2C promotes SAT lipid storage, and its reduction in obesity could contribute to fatty acid spillover and ectopic lipid accumulation. Of note, inhibition of cyclin-dependent kinase 6 (CDK6), another target of CDKN2C, improved glucose metabolism in mice with normal or high-

fat feeding (60). Proteins such as CDKN2C regulating the cell cycle, and EIF5 involved in translation initiation, were upregulated post surgery, suggesting enhanced cellular proliferation and protein synthesis. Cyclin-dependent kinase inhibitor 2 C (CDKN2C) inhibits cyclin-dependent kinase 4 and 6, thus functioning as a cell growth regulator that controls cell cycle G1 phase progression. CDKN2C also inhibits the cell cycle during adipocyte differentiation. Downregulation of CDKN2C in T2DM and obesity might contribute to reduced lipid storage in peripheral adipose tissue (62). *CDKN2C* mRNA expression in SAT was negatively correlated with hyperglycemia (HbA1C, fasting glucose, and glucose area under the curve (AUC) during OGTT) and with the insulin resistance markers homeostasis model assessment for insulin resistance (HOMA-IR), and free fatty acid (FFA) during OGTT, but positively with subcutaneous adipocyte insulin-stimulated glucose uptake ex vivo (62). The depletion of Eukaryotic Translation Initiation Factor 5 (EIF5) A1 is suggested to improve glucose intolerance and may also attenuate the dysfunction of pancreatic islets induced by pro-inflammatory cytokines (63).

The expression of profiles Kirsten Rat Sarcoma viral oncogene homolog (KRAS) and mammalian/mechanistic target of rapamycin complex (mTORC1) signaling pathways were downregulated after surgery. It has previously been shown that inhibition of KRAS enhanced adipogenic differentiation and adipogenesis in isolated adipocytes (64). Similarly, activated mTORC1 regulates adipogenesis, triglyceride synthesis, and mobilization in adipocytes (65). In addition, mTORC1 expression is consistently elevated in the adipose tissue of mice with diet-induced obesity, suggesting its role in adipose tissue expansion (66). The downregulation of these pathways postsurgery indicates a shift in adipose tissue composition, possibly involving the reduction in the lipid content and size of adipocytes (13). Peroxiredoxins (PRXS) are a ubiquitous family of antioxidant enzymes regulated by changes in phosphorylation, oxidation, reduction, and oligomerization (67). PRX3 and PRX5 suppress adipogenesis by regulating ROS generation and adipogenic gene expression (68).

Metabolic Adaptations and Regulation of Protein Synthesis

After bariatric surgery-induced weight loss, proteins associated with metabolic shifts and an enhanced capacity for protein synthesis, such as RPSA, AK2, and OGDH, showed increased expression. AK2 is a mitochondrial enzyme that catalyzes the transfer of a phosphoryl group from adenosine triphosphate (ATP) to adenosine monophosphate (AMP), producing adenosine diphosphate (ADP), and thus maintains the balance of adenine nucleotides in cells (69, 70). AK2 is markedly induced during adipocyte and B cell differentiation (69) and may be important for coupling ATP production in mitochondria with ATP utilization by the endoplasmic reticulum (ER) (69). The enzyme 2-oxoglutarate dehydrogenase (OGDH) is a key regulator in the TCA cycle and plays an important role in mitochondrial metabolism. A previous study suggested that OGDH activity in diabetic mice may be reduced (71), consistent with the observed upregulation post surgery associated with improved insulin sensitivity.

The downregulation of enzymes fundamental to lipid metabolism, including ACADL, ECHS1, ACADM, and DECR1, is of major significance in the current study. Acyl-coenzyme A dehydrogenase, long-chain (ACADL) catalyzes the initial step of fatty acid β-oxidation in mitochondria. CoA hydratase short-chain 1 (ECHS1) is a key mitochondrial enzyme involved in valine catabolism and fatty acid β-oxidation (72). Deficiency of ECHS1 usually leads to the accumulation of methacrylyl-CoA and acryloyl-CoA metabolites causing dysfunction of the pyruvate dehydrogenase (PDH) complex (73). PDH acts as a central metabolic node that mediates pyruvate oxidation after glycolysis and fuels the Krebs cycle to meet cellular energy demands (74). The suppressed expression of ACADM may be important in terms of the impaired fatty acid oxidation in obesity (75). DECR1 is a 2,4-dienoyl-CoA reductase that belongs to the short-chain dehydrogenase/reductase family. DECR1 is a rate-limiting enzyme in the polyunsaturated fatty acid β-oxidation accessory pathway, and elevated expression of DECR1 enhances lipolysis (76). Thus, the reduced expression of DECR1 possibly contributes to reduced fatty acid oxidation in obesity (77). The LRPPRC protein plays significant roles in energy metabolism by regulating the mitochondrial DNA-coded mRNAs (78) and promoting fatty acid uptake, oxidation, and oxidative phosphorylation (79) (see also *Regulation Mitochondrial Function and Oxidative Phosphorylation Pathway*). Its upregulation postsurgery is thus fully consistent with the recovery of mitochondrial function. The pitrilysin metallopeptidase 1 (PITRM1) is involved in the processing and degradation of peptides as they enter the mitochondrial matrix. Its increased expression postsurgery may thus play an important role in increasing mitochondrial functionality and efficiency in energy production (80), as failure to degrade these peptides is toxic for the mitochondria (80). Inorganic pyrophosphatase 1 (PPA1) catalyzes the hydrolysis of inorganic pyrophosphate to inorganic phosphate and is required for anabolism. A previous study found that overexpression of PPA1 in adipose tissue reversed obesity-associated metabolic disorders such as impaired glucose tolerance and severe insulin resistance in obese *PPA1* knockout mice (81). PPA1 deficiency results in mitochondrial dysfunction both in vitro and in vivo (81). Thus, the observed increase in PPA1 expression in obesity in our study might be a protective adaptation in conditions of excess energy availability.

Alterations in Cytoskeletal Proteins and Cellular Dynamics

Our study reveals an upregulation of proteins like TUBB4B and VIM in the SAT of persons with severe obesity. Tubulin β-4 b chain (TUBB4B) is essential for cell growth and development as a component of the microtubule network. The cytoskeleton undergoes significant rearrangements during adipogenesis and adipocyte hypertrophy (82). *VIM* gene encodes the type III intermediate filament protein vimentin, which is important for cell motility, migration, and endocytosis (83). In addition, vimentin forms cage-like structures around adipocyte lipid droplets and regulates their accumulation during adipogenesis (82). The downregulation of proteins involved in cytoskeletal organization and cellular dynamics (SPTAN1, CFL1, CAPZA1, and TUBB4B) may reflect changes in tissue structure and cellular

morphology and the return of SAT adipocyte size to normal following weight loss induced by surgery. Spectrin, α, nonerythrocytic 1 (SPTAN1) is a cytoskeletal protein involved in cellular functions such as DNA repair and cell cycle regulation. The expression of SPTAN1 was significantly higher in subcutaneous adipocytes of individuals with obesity with insulin resistance compared with their insulin-sensitive counterparts (84). SPTAN1 expression seems to be sensitive to hypoxia and associated with the dynamics of focal adhesions in adipose tissue remodeling, which may contribute to improved insulin sensitivity (85). Cofilin-1 (CFL1), a key regulator of the actin cytoskeleton, was found to be more highly expressed in the adipose tissue of mice with obesity, whereas its expression was lower in the group of animals resistant to obesity (86). Transcriptome analyses revealed the upregulation of *CFL1* in high-fat diet-induced hypertrophic adipocytes and its downregulation in brown/beige adipocytes (87). Considering the enzymatic activity of CFL1, its upregulation in hypertrophic adipocytes might be responsible for the subsequent attenuation of insulin-dependent glucose uptake (87). Thus, its reduction in the postsurgery biopsies may contribute to the increased AT insulin sensitivity under these conditions.

Regulation of Amino Acid Catabolic Pathways

We observed downregulation of aldehyde dehydrogenase 6 family member A1 (ALDH6A1), a key enzyme involved in cellular amino acid catabolism and the proximal enzyme in BCAA (leucine, isoleucine, and valine) catabolism, branched-chain transaminase 2 (BCAT2), in the adipose tissue of individuals with severe obesity. A previous study demonstrated that isolated adipocytes of individuals with diabetes showed reduced *ALDH6A1* gene expression (88). Considerable in vitro and ex vivo evidence suggests that adipose tissue is capable of metabolizing significant quantities of branched-chain amino acids (BCAAs) (89). BCAAs belong to the essential amino acids and their levels have earlier been reported to be elevated in plasma of individuals with obesity (90). Consistent with our findings, a previous study reported a reduction in BCAA catabolic enzyme activity in the adipose tissue of individuals with severe obesity and insulin resistance (91). In a previous mice study, adipose tissue-specific decrease in BCAA oxidation was associated with increased circulating BCAA levels (89). Because the mitochondrial BCAT2 is responsible for the reversible conversion of BCAAs into branched-chain α-ketoacids, its reduced expression may directly contribute to increased BCAA levels (89). A previous study found down-regulated pathways involving PCCA and PCCB in the adipose tissue of individuals with a high HOMA-IR (92). The upregulation of PCCA and PCCB after surgery thus has positive implications for metabolic pathways such as BCAA catabolism, propionate metabolism, glyoxylate, and dicarboxylate metabolism.

Conclusions

This study aimed to understand the complex mechanisms behind the adipose tissue dysfunction and metabolic complications in individuals with severe obesity, as well as the effects of weight loss achieved through bariatric surgery. The study found that several key proteins involved in mitochondrial integrity, RNA localization, amino acid catabolism, and lipid metabolism were decreased in individuals with severe obesity. Furthermore, enzymes that are essential for lipid metabolism were downregulated, suggesting impaired lipid processing in obesity. This dysfunction may contribute to excess fat accumulation and the health complications commonly associated with obesity. In contrast, proteins involved in cytoskeletal structure, cellular organization, and intercellular communication were more highly expressed in individuals with obesity. This may suggest a metabolic adaptation to cope with the increased volume of adipocytes.

Following bariatric surgery, expression of proteins associated with blood components, immune function, oxidative stress response, and metabolic pathways decreased, suggesting a potential reduction in chronic inflammation, improved insulin sensitivity, and an improvement in overall health post surgery. Conversely, bariatric surgery was associated with the upregulation of proteins involved in diverse cellular pathways and metabolic processes including mitochondrial function. These findings will enhance our understanding of the biological and molecular pathways driving weight gain and loss and could help researchers identify new therapeutic targets for obesity and metabolic diseases.

Limitations of the Study

This study has certain limitations. Some of the adipose tissue samples collected in this study were contaminated with blood. We therefore used serum protein depletion columns to remove the 12 most abundant serum components in the sample preparation step and employed a specialized scoring metric based on Human Protein Atlas and Human Blood Atlas to disqualify tissue samples containing highest blood-like protein signatures. The cutoff used to disqualify the samples with most blood contamination was selected by the researchers performing the analysis and is as such somewhat arbitrary. On the contrary, using this method to filter out the most contaminated is still more objective and transparent than evaluating the blood contamination visually by color. Furthermore, filtering out data from the bloodiest adipose tissue samples reduced the number of samples available for analysis. Having a higher number of samples available might have confirmed the trends for improvement seen after bariatric surgery. Furthermore, the bariatric surgery was performed after a 4-wk very low-calorie diet as is required to reduce the risk surgery complications. Thus, the diet may have caused some bias when comparing the baseline proteome from the patients with those from controls who did not have the diet. Specifically, previous studies have shown a considerable reduction on mitochondrial function with diet-induced weight loss (93–95). However, these studies had a larger, 10%–14% weight-loss compared with 7% in our study. It is thus likely that this weight loss effect has been smaller in our study.

DATA AVAILABILITY

The mass spectrometry proteomics data have been deposited to the ProteomeXchange Consortium via the PRIDE (96) partner repository with the dataset identifier PXD034182. Any additional information required to reanalyze the data reported in this paper

is available from the corresponding author upon reasonable request.

SUPPLEMENTAL MATERIAL

Supplemental Files S1, *A–C* and S2, *A–C*, Supplemental Table S1, and Supplemental Fig. S1: https://doi.org/10.6084/m9.figshare.c.7581680.v1.

ACKNOWLEDGMENTS

This work was conducted within the Finnish Centre of Excellence in Molecular Imaging in Cardiovascular and Metabolic Research. Mass spectrometry analysis was performed at the Turku Proteomics Facility, University of Turku, and Åbo Akademi University.

GRANTS

This work was supported by the Academy of Finland (Grant No. 307402 to P.N.), the University of Turku, University Hospital, Åbo Akademi University (Finland). P.D. received funding from the Finnish Medical Association, the Finnish Diabetes Research Foundation, Finnish Cultural Foundation, Finnish-Norwegian Medical Foundation, Instrumentarium Science Foundation, Päivikki and Sakari Sohlberg Foundation, the Onni and Hilja Tuovinen Foundation, Jalmari and Rauha Ahokas Foundation, and Aarne Koskelo Foundation. M.-J.H. was supported by the Finnish Diabetes Research Foundation and the Academy of Finland (Grant 332151). A. Roivainen and S.P. were supported by the Academy of Finland (Grant 335975). P.J. received a Finnish Distinguished Professorship from TEKES and the Academy of Finland. The Turku Proteomics Facility is supported by Biocenter Finland. The group of V.M.O. was supported by the Academy of Finland (Grant 322647), the Sigrid Jusélius Foundation, the Liv och Hälsa Foundation, the Finnish Diabetes Research Foundation, Diabetes Wellness Finland, the Magnus Ehrnrooth Foundation, Finnish Society of Sciences and Letters and Jane and Aatos Erkko Foundation. L.L.E. reports grants from the European Research Council ERC (677943), European Union's Horizon 2020 research and innovation programme (955321), Academy of Finland (310561, 314443, 329278, 335434, 335611, and 341342), and Sigrid Juselius Foundation during the conduct of the study. Our research is also supported by Biocenter Finland and ELIXIR Finland.

DISCLAIMERS

The funding agencies did not participate in study design, collection, analysis, or interpretation of data, writing of the report, nor the decision to submit the article for publication.

DISCLOSURES

All authors have read the journal's authorship agreement and policy on disclosure of conflicts of interest and declare no potential conflicts of interest.

AUTHOR CONTRIBUTIONS

P.D., M.-J.H., P.A.N.H., A. Rokka, A. Roivainen, P.S., P.J., V.M.O., L.L.E., and P.N. conceived and designed research; A. Rokka, S.P., E.G., P.S., and P.J. performed experiments; P.D., M.-J.H., T.S., A. Rokka, E.G., and N.W. analyzed data; P.D., M.-J.H., T.S., P.A.N.H., S.P., A. Roivainen, P.S., V.M.O., L.L.E., and P.N. interpreted results of experiments; M.-J.H., T.S., and P.A.N.H. prepared figures; P.D. drafted manuscript; P.D., M.-J.H., T.S., P.A.N.H., A. Roivainen, P.S., V.M.O., L.L.E., and P.N. edited and revised manuscript; P.D., M.-J.H., T.S., P.A.N.H., A. Rokka, S.P., E.G., N.W., A. Roivainen, P.S., P.J., V.M.O., L.L.E., and P.N. approved final version of manuscript.

REFERENCES

1. **Hruby A**, **Hu FB.** The epidemiology of obesity: a big picture. *Pharmacoeconomics* 33: 673–689, 2015. doi:10.1007/s40273-014-0243-x.
2. **Chait A**, **den Hartigh LJ.** Adipose tissue distribution, inflammation and its metabolic consequences, including diabetes and cardiovascular disease. *Front Cardiovasc Med* 7: 22, 2020. doi:10.3389/fcvm.2020.00022.
3. **Trayhurn P.** Endocrine and signalling role of adipose tissue: new perspectives on fat. *Acta Physiol Scand* 184: 285–293, 2005. doi:10.1111/j.1365-201X.2005.01468.x.
4. **Baker AR**, **Silva NF**, **Quinn DW**, **Harte AL**, **Pagano D**, **Bonser RS**, **Kumar S**, **McTernan PG.** Human epicardial adipose tissue expresses a pathogenic profile of adipocytokines in patients with cardiovascular disease. *Cardiovasc Diabetol* 5: 1, 2006. doi:10.1186/1475-2840-5-1.
5. **Matsuzawa Y**, **Shimomura I**, **Nakamura T**, **Keno Y**, **Kotani K**, **Tokunaga K.** Pathophysiology and pathogenesis of visceral fat obesity. *Obes Res* 3, *Suppl* 2: 187S–194S, 1995. doi:10.1002/j.1550-8528.1995.tb00462.x.
6. **Hajer GR**, **van Haeften TW**, **Visseren FLJ.** Adipose tissue dysfunction in obesity, diabetes, and vascular diseases. *Eur Heart J* 29: 2959–2971, 2008. doi:10.1093/eurheartj/ehn387.
7. **Jo J**, **Gavrilova O**, **Pack S**, **Jou W**, **Mullen S**, **Sumner AE**, **Cushman SW**, **Periwal V.** Hypertrophy and/or hyperplasia: dynamics of adipose tissue growth. *PLoS Comput Biol* 5: e1000324, 2009. doi:10.1371/journal.pcbi.1000324.
8. **Osellame LD**, **Blacker TS**, **Duchen MR.** Cellular and molecular mechanisms of mitochondrial function. *Best Pract Res Clin Endocrinol Metab* 26: 711–723, 2012. doi:10.1016/j.beem.2012.05.003.
9. **Cheng Z**, **Ristow M.** Mitochondria and metabolic homeostasis. *Antioxid Redox Signal* 19: 240–242, 2013. doi:10.1089/ars.2013.5255.
10. **Starkov AA.** The role of mitochondria in reactive oxygen species metabolism and signaling. *Ann N Y Acad Sci* 1147: 37–52, 2008. doi:10.1196/annals.1427.015.
11. **Gao AW**, **Cantó C**, **Houtkooper RH.** Mitochondrial response to nutrient availability and its role in metabolic disease. *EMBO Mol Med* 6: 580–589, 2014. doi:10.1002/emmm.201303782.
12. **Salminen P**, **Grönroos S**, **Helmiö M**, **Hurme S**, **Juuti A**, **Juusela R**, **Peromaa-Haavisto P**, **Leivonen M**, **Nuutila P**, **Ovaska J.** Effect of laparoscopic sleeve gastrectomy vs roux-en-Y gastric bypass on weight loss, comorbidities, and reflux at 10 years in adult patients with obesity: the SLEEVEPASS randomized clinical trial. *JAMA Surg* 157: 656–666, 2022. doi:10.1001/jamasurg.2022.2229.
13. **Frikke-Schmidt H**, **O'Rourke RW**, **Lumeng CN**, **Sandoval DA**, **Seeley RJ.** Does bariatric surgery improve adipose tissue function? *Obes Rev Off Rev* 17: 795–809, 2016. doi:10.1111/obr.12429.
14. **Schauer PR**, **Bhatt DL**, **Kirwan JP**, **Wolski K**, **Aminian A**, **Brethauer SA**, **Navaneethan SD**, **Singh RP**, **Pothier CE**, **Nissen SE**, **Kashyap SR**; **STAMPEDE Investigators.** Bariatric surgery versus intensive medical therapy for diabetes - 5-year outcomes. *N Engl J Med* 376: 641–651, 2017. doi:10.1056/NEJMoa1600869.
15. **Dadson P**, **Honka MJ**, **Suomi T**, **Haridas PAN**, **Rokka A**, **Palani S**, **Goltseva E**, **Wang N**, **Roivainen A**, **Salminen P**, **James P**, **Olkkonen VM**, **Elo LL**, **Nuutila P.** Supplementary material for Proteomic Profiling Reveals Alterations in Metabolic and Cellular Pathways in Severe Obesity and Following Bariatric Surgery [Internet]. figshare. https://doi.org/10.6084/m9.figshare.c.7581680 [2024 Dec 18].
16. **Hannukainen JC**, **Lautamäki R**, **Pärkkä J**, **Strandberg M**, **Saunavaara V**, **Hurme S**, **Soinio M**, **Dadson P**, **Virtanen KA**, **Grönroos T**, **Forsback S**, **Salminen P**, **Iozzo P**, **Nuutila P.** Reversibility of myocardial metabolism and remodelling in morbidly obese patients 6 months after bariatric surgery. *Diabetes Obes Metab* 20: 963–973, 2018. doi:10.1111/dom.13183.
17. **Wallace TM**, **Levy JC**, **Matthews DR.** Use and abuse of HOMA modeling. *Diabetes Care* 27: 1487–1495, 2004. doi:10.2337/diacare.27.6.1487.
18. **Dadson P**, **Ferrannini E**, **Landini L**, **Hannukainen JC**, **Kalliokoski KK**, **Vaittinen M**, **Honka H**, **Karlsson HK**, **Tuulari JJ**, **Soinio M**, **Salminen P**, **Parkkola R**, **Pihlajamäki J**, **Iozzo P**, **Nuutila P.** Fatty acid uptake and blood flow in adipose tissue compartments of

morbidly obese subjects with or without type 2 diabetes: effects of bariatric surgery. *Am J Physiol Endocrinol Physiol* 313: E175–E182, 2017. doi:10.1152/ajpendo.00044.2017.

19. **Dadson P**, **Landini L**, **Helmiö M**, **Hannukainen JC**, **Immonen H**, **Honka M-J**, **Bucci M**, **Savisto N**, **Soinio M**, **Salminen P**, **Parkkola R**, **Pihlajamäki J**, **Iozzo P**, **Ferrannini E**, **Nuutila P.** Effect of bariatric surgery on adipose tissue glucose metabolism in different depots in patients with or without type 2 diabetes. *Diabetes Care* 39: 292–299, 2016. doi:10.2337/dc15-1447.
20. **Schrauwen P**, **Wagenmakers AJ**, **van Marken Lichtenbelt WD**, **Saris WH**, **Westerterp KR.** Increase in fat oxidation on a high-fat diet is accompanied by an increase in triglyceride-derived fatty acid oxidation. *Diabetes* 49: 640–646, 2000. doi:10.2337/diabetes.49.4.640.
21. **Weir JBDB.** New methods for calculating metabolic rate with special reference to protein metabolism. *J Physiol* 109: 1–9, 1949. doi:10.1113/jphysiol.1949.sp004363.
22. **Hoffstedt J**, **Andersson DP**, **Eriksson Hogling D**, **Theorell J**, **Näslund E**, **Thorell A**, **Ehrlund A**, **Rydén M**, **Arner P.** Long-term protective changes in adipose tissue after gastric bypass. *Diabetes Care* 40: 77–84, 2017. doi:10.2337/dc16-1072.
23. **Tyanova S**, **Temu T**, **Cox J.** The MaxQuant computational platform for mass spectrometry-based shotgun proteomics. *Nat Protoc* 11: 2301–2319, 2016. doi:10.1038/nprot.2016.136.
24. **Huber W**, **von Heydebreck A**, **Sültmann H**, **Poustka A**, **Vingron M.** Variance stabilization applied to microarray data calibration and to the quantification of differential expression. *Bioinformatics* 18, *Suppl* 1: S96–104, 2002. doi:10.1093/bioinformatics/18.suppl_1.s96.
25. **Uhlén M**, **Fagerberg L**, **Hallström BM**, **Lindskog C**, **Oksvold P**, **Mardinoglu A**, **et al.** Tissue-based map of the human proteome. *Science* 347: 1260419, 2015. doi:10.1126/science.1260419.
26. **Uhlen M**, **Karlsson MJ**, **Zhong W**, **Tebani A**, **Pou C**, **Mikes J**, **Lakshmikanth T**, **Forsström B**, **Edfors F**, **Odeberg J**, **Mardinoglu A**, **Zhang C**, **von Feilitzen K**, **Mulder J**, **Sjöstedt E**, **Hober A**, **Oksvold P**, **Zwahlen M**, **Ponten F**, **Lindskog C**, **Sivertsson Å**, **Fagerberg L**, **Brodin P.** A genome-wide transcriptomic analysis of protein-coding genes in human blood cells. *Science* 366: eaax9198, 2019. doi:10.1126/science.aax9198.
27. **Subramanian A**, **Tamayo P**, **Mootha VK**, **Mukherjee S**, **Ebert BL**, **Gillette MA**, **Paulovich A**, **Pomeroy SL**, **Golub TR**, **Lander ES**, **Mesirov JP.** Gene set enrichment analysis: a knowledge-based approach for interpreting genome-wide expression profiles. *Proc Natl Acad Sci USA* 102: 15545–15550, 2005. doi:10.1073/pnas.0506580102.
28. **Suomi T**, **Seyednasrollah F**, **Jaakkola MK**, **Faux T**, **Elo LL.** ROTS: an R package for reproducibility-optimized statistical testing. *PLoS Comput Biol* 13: e1005562, 2017. doi:10.1371/journal.pcbi.1005562.
29. **Fröhlich K**, **Brombacher E**, **Fahrner M**, **Vogele D**, **Kook L**, **Pinter N**, **Bronsert P**, **Timme-Bronsert S**, **Schmidt A**, **Bärenfaller K**, **Kreutz C**, **Schilling O.** Benchmarking of analysis strategies for data-independent acquisition proteomics using a large-scale dataset comprising inter-patient heterogeneity. *Nat Commun* 13: 2622, 2022. doi:10.1038/s41467-022-30094-0.
30. **Peng H**, **Wang H**, **Kong W**, **Li J**, **Goh WWB.** Optimizing differential expression analysis for proteomics data via high-performing rules and ensemble inference. *Nat Commun* 15: 3922, 2024. doi:10.1038/s41467-024-47899-w.
31. **Lin MH**, **Wu PS**, **Wong TH**, **Lin IY**, **Lin J**, **Cox J**, **Yu SH.** Benchmarking differential expression, imputation and quantification methods for proteomics data. *Brief Bioinform* 23: bbac138, 2022. doi:10.1093/bib/bbac138.
32. **Korotkevich G**, **Sukhov V**, **Budin N**, **Shpak B**, **Artyomov MN**, **Sergushichev A.** Fast gene set enrichment analysis (Preprint). *bioRxiv* 060012, 2021. doi:10.1101/060012.
33. **Gu Z**, **Eils R**, **Schlesner M.** Complex heatmaps reveal patterns and correlations in multidimensional genomic data. *Bioinformatics* 32: 2847–2849, 2016. doi:10.1093/bioinformatics/btw313.
34. **Benjamini Y**, **Hochberg Y.** Controlling the false discovery rate: a practical and powerful approach to multiple testing. *J R Stat Soc Ser B Methodol* 57: 289–300, 1995. doi:10.1111/j.2517-6161.1995.tb02031.x.
35. **Immonen H**, **Hannukainen JC**, **Kudomi N**, **Pihlajamäki J**, **Saunavaara V**, **Laine J**, **Salminen P**, **Lehtimäki T**, **Pham T**, **Iozzo P**, **Nuutila P.** Increased liver fatty acid uptake is partly reversed and liver fat content normalized after bariatric surgery. *Diabetes Care* 41: 368–371, 2018. doi:10.2337/dc17-0738.
36. **Oláhová M**, **Hardy SA**, **Hall J**, **Yarham JW**, **Haack TB**, **Wilson WC**, **Alston CL**, **He L**, **Aznauryan E**, **Brown RM**, **Brown GK**, **Morris AA**, **Mundy H**, **Broomfield A**, **Barbosa IA**, **Simpson MA**, **Deshpande C**, **Moeslinger D**, **Koch J**, **Stettner GM**, **Bonnen PE**, **Prokisch H**, **Lightowlers RN**, **McFarland R**, **Chrzanowska-Lightowlers ZM**, **Taylor RW.** LRPPRC mutations cause early-onset multisystem mitochondrial disease outside of the French-Canadian population. *Brain* 138: 3503–3519, 2015. doi:10.1093/brain/awv291.
37. **Sasarman F**, **Nishimura T**, **Antonicka H**, **Weraarpachai W**, **Shoubridge EA**, **Allen B**; **LSFC Consortium.** Tissue-specific responses to the LRPPRC founder mutation in French Canadian Leigh Syndrome. *Hum Mol Genet*. 24: 480–491, 2015. doi:10.1093/hmg/ddu468.
38. **Nam M**, **Akie TE**, **Sanosaka M**, **Craige SM**, **Kant S**, **Keaney JF**, **Cooper MP.** Mitochondrial retrograde signaling connects respiratory capacity to thermogenic gene expression. *Sci Rep* 7: 2013, 2017. doi:10.1038/s41598-017-01879-x.
39. **Mardinoglu A**, **Heiker JT**, **Gärtner D**, **Björnson E**, **Schön MR**, **Flehmig G**, **Klöting N**, **Krohn K**, **Fasshauer M**, **Stumvoll M**, **Nielsen J**, **Blüher M.** Extensive weight loss reveals distinct gene expression changes in human subcutaneous and visceral adipose tissue. *Sci Rep* 5: 14841, 2015. doi:10.1038/srep14841.
40. **Wongkittichote P**, **Ah Mew NA**, **Chapman KA.** Propionyl-CoA carboxylase- A review. *Mol Genet Metab* 122: 145–152, 2017. doi:10.1016/j.ymgme.2017.10.002.
41. **Fazakerley DJ**, **Chaudhuri R**, **Yang P**, **Maghzal GJ**, **Thomas KC**, **Krycer JR**, **Humphrey SJ**, **Parker BL**, **Fisher-Wellman KH**, **Meoli CC**, **Hoffman NJ**, **Diskin C**, **Burchfield JG**, **Cowley MJ**, **Kaplan W**, **Modrusan Z**, **Kolumam G**, **Yang JY**, **Chen DL**, **Samocha-Bonet D**, **Greenfield JR**, **Hoehn KL**, **Stocker R**, **James DE.** Mitochondrial CoQ deficiency is a common driver of mitochondrial oxidants and insulin resistance. *eLife* 7: e32111, 2018. doi:10.7554/eLife.32111.
42. **Loh K**, **Deng H**, **Fukushima A**, **Cai X**, **Boivin B**, **Galic S**, **Bruce C**, **Shields BJ**, **Skiba B**, **Ooms LM**, **Stepto N**, **Wu B**, **Mitchell CA**, **Tonks NK**, **Watt MJ**, **Febbraio MA**, **Crack PJ**, **Andrikopoulos S**, **Tiganis T.** Reactive oxygen species enhance insulin sensitivity. *Cell Metab* 10: 260–272, 2009. doi:10.1016/j.cmet.2009.08.009.
43. **Katsouda A**, **Valakos D**, **Dionellis VS**, **Bibli SI**, **Akoumianakis I**, **Karaliota S**, **Zuhra K**, **Fleming I**, **Nagahara N**, **Havaki S**, **Gorgoulis VG**, **Thanos D**, **Antoniades C**, **Szabo C**, **Papapetropoulos A.** MPST sulfurtransferase maintains mitochondrial protein import and cellular bioenergetics to attenuate obesity. *J Exp Med* 219: e20211894, 2022. doi:10.1084/jem.20211894.
44. **Comas F**, **Latorre J**, **Ortega F**, **Arnoriaga Rodríguez M**, **Lluch A**, **Sabater M**, **Rius F**, **Ribas X**, **Costas M**, **Ricart W**, **Lecube A**, **Fernández-Real JM**, **Moreno-Navarrete JM.** Morbidly obese subjects show increased serum sulfide in proportion to fat mass. *Int J Obes (Lond)* 45: 415–426, 2021. doi:10.1038/s41366-020-00696-z.
45. **Latorre J**, **Aroca A**, **Fernández-Real JM**, **Romero LC**, **Moreno-Navarrete JM.** The combined partial knockdown of CBS and MPST genes induces inflammation, impairs adipocyte function-related gene expression and disrupts protein persulfidation in human adipocytes. *Antioxidants* 11: 1095, 2022. doi:10.3390/antiox11061095.
46. **Siegel D**, **Gustafson DL**, **Dehn DL**, **Han JY**, **Boonchoong P**, **Berliner LJ**, **Ross D.** NAD(P)H:quinone oxidoreductase 1: role as a superoxide scavenger. *Mol Pharmacol* 65: 1238–1247, 2004. doi:10.1124/mol.65.5.1238.
47. **Palming J**, **Sjöholm K**, **Jernås M**, **Lystig TC**, **Gummesson A**, **Romeo S**, **Lönn L**, **Lönn M**, **Carlsson B**, **Carlsson LMS.** The expression of NAD(P)H:quinone oxidoreductase 1 is high in human adipose tissue, reduced by weight loss, and correlates with adiposity, insulin sensitivity, and markers of liver dysfunction. *J Clin Endocrinol Metab* 92: 2346–2352, 2007. doi:10.1210/jc.2006-2476.
48. **Hwang JH**, **Kim DW**, **Jo EJ**, **Kim YK**, **Jo YS**, **Park JH**, **Yoo SK**, **Park MK**, **Kwak TH**, **Kho YL**, **Han J**, **Choi HS**, **Lee SH**, **Kim JM**, **Lee IKyu**, **Kyung T**, **Jang C**, **Chung J**, **Kweon GR**, **Shong M.** Pharmacological stimulation of NADH oxidation ameliorates obesity and related phenotypes in mice. *Diabetes* 58: 965–974, 2009. doi:10.2337/db08-1183.
49. **Kim YH**, **Hwang JH**, **Kim KS**, **Noh JR**, **Gang GT**, **Oh WK**, **Jeong KH**, **Kwak TH**, **Choi HS**, **Lee IK**, **Lee CH.** Enhanced activation of NAD(P)H: quinone oxidoreductase 1 attenuates spontaneous hypertension by improvement of endothelial nitric oxide synthase coupling via tumor suppressor kinase liver kinase B1/adenosine 5'-monophosphate-activated protein kinase-mediated guanosine 5'-triphosphate

cyclohydrolase 1 preservation. *J Hypertens* 32: 306–317, 2014. doi:10.1097/HJH.0000000000000018.

50. **Grande R**, **Dovizio M**, **Marcone S**, **Szklanna PB**, **Bruno A**, **Ebhardt HA**, **Cassidy H**, **Ní Áinle F**, **Caprodossi A**, **Lanuti P**, **Marchisio M**, **Mingrone G**, **Maguire PB**, **Patrignani P.** Platelet-derived microparticles from obese individuals: characterization of number, size, proteomics, and crosstalk with cancer and endothelial cells. *Front Pharmacol* 10: 7, 2019. doi:10.3389/fphar.2019.00007.
51. **Norman-Burgdolf H**, **Li D**, **Sullivan P**, **Wang S.** CD47 differentially regulates white and brown fat function. *Biol Open* 9: bio056747, 2020. doi:10.1242/bio.056747.
52. **Li D**, **Gwag T**, **Wang S.** Absence of CD47 maintains brown fat thermogenic capacity and protects mice from aging-related obesity and metabolic disorder. *Biochem Biophys Res Commun* 575: 14–19, 2021. doi:10.1016/j.bbrc.2021.08.062.
53. **Maimaitiyiming H**, **Norman H**, **Zhou Q**, **Wang S.** CD47 deficiency protects mice from diet-induced obesity and improves whole body glucose tolerance and insulin sensitivity. *Sci Rep* 5: 8846, 2015. doi:10.1038/srep08846.
54. **Deng T**, **Lyon CJ**, **Minze LJ**, **Lin J**, **Zou J**, **Liu JZ**, **Ren Y**, **Yin Z**, **Hamilton DJ**, **Reardon PR**, **Sherman V**, **Wang HY**, **Phillips KJ**, **Webb P**, **Wong STC**, **Wang RF**, **Hsueh WA.** Class II major histocompatibility complex plays an essential role in obesity-induced adipose inflammation. *Cell Metab* 17: 411–422, 2013. doi:10.1016/j.cmet.2013.02.009.
55. **Wang Q**, **Wang Y**, **Xu D.** The roles of T cells in obese adipose tissue inflammation. *Adipocyte*. 10: 435–445, 2021. doi:10.1080/21623945.2021.1965314.
56. **Ballanti E**, **Perricone C**, **Greco E**, **Ballanti M**, **Di Muzio G**, **Chimenti MS**, **Perricone R.** Complement and autoimmunity. *Immunol Res* 56: 477–491, 2013. doi:10.1007/s12026-013-8422-y.
57. **Engström G**, **Hedblad B**, **Eriksson KF**, **Janzon L**, **Lindgärde F.** Complement C3 is a risk factor for the development of diabetes: a population-based cohort study. *Diabetes* 54: 570–575, 2005. doi:10.2337/diabetes.54.2.570.
58. **Gragnoli C.** Overweight condition and waist circumference and a candidate gene within the 12q24 locus. *Cardiovasc Diabetol* 12: 2, 2013. doi:10.1186/1475-2840-12-2.
59. **Ceperuelo-Mallafré V**, **Ejarque M**, **Serena C**, **Duran X**, **Montori-Grau M**, **Rodríguez MA**, **Yanes O**, **Núñez-Roa C**, **Roche K**, **Puthanveetil P**, **Garrido-Sánchez L**, **Saez E**, **Tinahones FJ**, **Garcia-Roves PM**, **Gómez-Foix AM**, **Saltiel AR**, **Vendrell J**, **Fernández-Veledo S.** Adipose tissue glycogen accumulation is associated with obesity-linked inflammation in humans. *Mol Metab* 5: 5–18, 2016. doi:10.1016/j.molmet.2015.10.001.
60. **Hou X**, **Zhang Y**, **Li W**, **Hu AJ**, **Luo C**, **Zhou W**, **Hu JK**, **Daniele SG**, **Wang J**, **Sheng J**, **Fan Y**, **Greenberg AS**, **Farmer SR**, **Hu MG.** CDK6 inhibits white to beige fat transition by suppressing RUNX1. *Nat Commun* 9: 1023, 2018. doi:10.1038/s41467-018-03451-1.
61. **Viguerie N**, **Montastier E**, **Maoret JJ**, **Roussel B**, **Combes M**, **Valle C**, **Villa-Vialaneix N**, **Iacovoni JS**, **Martinez JA**, **Holst C**, **Astrup A**, **Vidal H**, **Clément K**, **Hager J**, **Saris WH**, **Langin D.** Determinants of human adipose tissue gene expression: impact of diet, sex, metabolic status, and cis genetic regulation. *PLoS Genet* 8: e1002959, 2012. doi:10.1371/journal.pgen.1002959.
62. **Pereira MJ**, **Vranic M**, **Kamble PG**, **Jernow H**, **Kristófi R**, **Holbikova E**, **Skrtic S**, **Kullberg J**, **Svensson MK**, **Hetty S**, **Eriksson JW.** CDKN2C expression in adipose tissue is reduced in type II diabetes and central obesity: impact on adipocyte differentiation and lipid storage? *Transl Res* 242: 105–121, 2022. doi:10.1016/j.trsl.2021.12.003.
63. **Maier B**, **Ogihara T**, **Trace AP**, **Tersey SA**, **Robbins RD**, **Chakrabarti SK**, **Nunemaker CS**, **Stull ND**, **Taylor CA**, **Thompson JE**, **Dondero RS**, **Lewis EC**, **Dinarello CA**, **Nadler JL**, **Mirmira RG.** The unique hypusine modification of eIF5A promotes islet beta cell inflammation and dysfunction in mice. *J Clin Invest* 120: 2156–2170, 2010. doi:10.1172/JCI38924.
64. **Yu W**, **Chen CZ**, **Peng Y**, **Li Z**, **Gao Y**, **Liang S**, **Yuan B**, **Kim NH**, **Jiang H**, **Zhang JB.** KRAS affects adipogenic differentiation by regulating autophagy and MAPK activation in 3T3-L1 and C2C12 cells. *Int J Mol Sci* 22: 13630, 2021. doi:10.3390/ijms222413630.
65. **Ricoult SJ**, **Manning BD.** The multifaceted role of mTORC1 in the control of lipid metabolism. *EMBO Rep* 14: 242–251, 2013. doi:10.1038/embor.2013.5.
66. **Um SH**, **Frigerio F**, **Watanabe M**, **Picard F**, **Joaquin M**, **Sticker M**, **Fumagalli S**, **Allegrini PR**, **Kozma SC**, **Auwerx J**, **Thomas G.** Absence of S6K1 protects against age- and diet-induced obesity while enhancing insulin sensitivity. *Nature* 431: 200–205, 2004. doi:10.1038/nature02866.
67. **Wood ZA**, **Schröder E**, **Robin Harris J**, **Poole LB.** Structure, mechanism and regulation of peroxiredoxins. *Trends Biochem Sci* 28: 32–40, 2003. doi:10.1016/s0968-0004(02)00003-8.
68. **Kim JH**, **Park SJ**, **Chae U**, **Seong J**, **Lee HS**, **Lee SR**, **Lee S**, **Lee DS.** Peroxiredoxin 2 mediates insulin sensitivity of skeletal muscles through regulation of protein tyrosine phosphatase oxidation. *Int J Biochem Cell Biol* 99: 80–90, 2018. doi:10.1016/j.biocel.2018.03.019.
69. **Burkart A**, **Shi X**, **Chouinard M**, **Corvera S.** Adenylate kinase 2 links mitochondrial energy metabolism to the induction of the unfolded protein response. *J Biol Chem* 286: 4081–4089, 2011. doi:10.1074/jbc.M110.134106.
70. **Ghaloul-Gonzalez L**, **Mohsen A-W**, **Karunanidhi A**, **Seminotti B**, **Chong H**, **Madan-Khetarpal S**, **Sebastian J**, **Vockley CW**, **Reyes-Múgica M**, **Vander Lugt MT**, **Vockley J.** Reticular dysgenesis and mitochondriopathy induced by adenylate kinase 2 deficiency with atypical presentation. *Sci Rep* 9: 15739, 2019. doi:10.1038/s41598-019-51922-2.
71. **Yu Q**, **Liu B**, **Ruan D**, **Niu C**, **Shen J**, **Ni M**, **Cong W**, **Lu X**, **Jin L.** A novel targeted proteomics method for identification and relative quantitation of difference in nitration degree of OGDH between healthy and diabetic mouse. *Proteomics* 14: 2417–2426, 2014. doi:10.1002/pmic.201400274.
72. **Pata S**, **Flores-Rojas K**, **Gil A**, **López-Laso E**, **Marti-Sánchez L**, **Baide-Mairena H**, **Pérez-Dueñas B**, **Gil-Campos M.** Clinical improvements after treatment with a low-valine and low-fat diet in a pediatric patient with enoyl-CoA hydratase, short chain 1 (ECHS1) deficiency. *Orphanet J Rare Dis* 17: 340, 2022. doi:10.1186/s13023-022-02468-6.
73. **Olgiati S**, **Skorvanek M**, **Quadri M**, **Minneboo M**, **Graafland J**, **Breedveld GJ**, **Bonte R**, **Ozgur Z**, **van den Hout MC**, **Schoonderwoerd K**, **Verheijen FW**, **van IJcken WF**, **Chien HF**, **Barbosa ER**, **Chang HC**, **Lai SC**, **Yeh TH**, **Lu CS**, **Wu-Chou YH**, **Kievit AJ**, **Han V**, **Gdovinova Z**, **Jech R**, **Hofstra RMW**, **Ruijter GJ**, **Mandemakers W**, **Bonifati V.** Paroxysmal exercise-induced dystonia within the phenotypic spectrum of ECHS1 deficiency. *Mov Disord Off Disord* 31: 1041–1048, 2016. doi:10.1002/mds.26610.
74. **Park S**, **Jeon JH**, **Min BK**, **Ha CM**, **Thoudam T**, **Park BY**, **Lee IK.** Role of the pyruvate dehydrogenase complex in metabolic remodeling: differential pyruvate dehydrogenase complex functions in metabolism. *Diabetes Metab J* 42: 270–281, 2018. doi:10.4093/dmj.2018.0101.
75. **Zhu JY**, **Chen M**, **Mu WJ**, **Luo HY**, **Guo L.** Higd1a facilitates exercise-mediated alleviation of fatty liver in diet-induced obese mice. *Metabolism* 134: 155241, 2022. doi:10.1016/j.metabol.2022.155241.
76. **Zhou H**, **Zhang J**, **Yan Z**, **Qu M**, **Zhang G**, **Han J**, **Wang F**, **Sun K**, **Wang L**, **Yang X.** DECR1 directly activates HSL to promote lipolysis in cervical cancer cells. *Biochim Biophys Acta Mol Cell Biol Lipids* 1867: 159090, 2022. doi:10.1016/j.bbalip.2021.159090.
77. **Karpe F**, **Dickmann JR**, **Frayn KN.** Fatty acids, obesity, and insulin resistance: time for a reevaluation. *Diabetes* 60: 2441–2449, 2011. doi:10.2337/db11-0425.
78. **Cui J**, **Wang L**, **Ren X**, **Zhang Y**, **Zhang H.** LRPPRC: a multifunctional protein involved in energy metabolism and human disease. *Front Physiol* 10: 595, 2019. doi:10.3389/fphys.2019.00595.
79. **Lei S**, **Sun RZ**, **Wang D**, **Gong MZ**, **Su -P**, **Yi F**, **Peng ZW.** Increased hepatic fatty acids uptake and oxidation by LRPPRC-driven oxidative phosphorylation reduces blood lipid levels. *Front Physiol* 7: 270, 2016. doi:10.3389/fphys.2016.00270.
80. **Ehrich TH**, **Hrbek T**, **Kenney-Hunt JP**, **Pletscher LS**, **Wang B**, **Semenkovich CF**, **Cheverud JM.** Fine-mapping gene-by-diet interactions on chromosome 13 in a LG/J × SM/J murine model of obesity. *Diabetes* 54: 1863–1872, 2005. doi:10.2337/diabetes.54.6.1863.
81. **Yin Y**, **Wu Y**, **Zhang X**, **Zhu Y**, **Sun Y**, **Yu J**, **Gong Y**, **Sun P**, **Lin H**, **Han X.** PPA1 regulates systemic insulin sensitivity by maintaining adipocyte mitochondria function as a novel PPARγ target gene. *Diabetes* 70: 1278–1291, 2021. doi:10.2337/db20-0622.
82. **Verstraeten VL**, **Renes J**, **Ramaekers FCS**, **Kamps M**, **Kuijpers HJ**, **Verheyen F**, **Wabitsch M**, **Steijlen PM**, **van Steensel MA**, **Broers JL.** Reorganization of the nuclear lamina and cytoskeleton in adipogenesis. *Histochem Cell Biol* 135: 251–261, 2011. doi:10.1007/s00418-011-0792-4.

83. **de Pablo Y**, **Nilsson M**, **Pekna M**, **Pekny M.** Intermediate filaments are important for astrocyte response to oxidative stress induced by oxygen–glucose deprivation and reperfusion. *Histochem Cell Biol* 140: 81–91, 2013. doi:10.1007/s00418-013-1110-0.
84. **Xie X**, **Yi Z**, **Sinha S**, **Madan M**, **Bowen BP**, **Langlais P**, **Ma D**, **Mandarino L**, **Meyer C.** Proteomics analyses of subcutaneous adipocytes reveal novel abnormalities in human insulin resistance. *Obesity (Silver Spring)* 24: 1506–1514, 2016. doi:10.1002/oby.21528.
85. **Van Meijel RLJ**, **Wang P**, **Bouwman F**, **Blaak EE**, **Mariman ECM**, **Goossens GH.** The effects of mild intermittent hypoxia exposure on the abdominal subcutaneous adipose tissue proteome in overweight and obese men: a first-in-human randomized, single-blind, and cross-over study. *Front Physiol* 12: 791588, 2021. doi:10.3389/fphys.2021.791588.
86. **Kim SW**, **Park TJ**, **Choi JH**, **Aseer KR**, **Choi JY**, **Kim YJ**, **Choi MS**, **Yun JW.** Differential protein expression in white adipose tissue from obesity-prone and obesity-resistant mice in response to high fat diet and anti-obesity herbal medicines. *Cell Physiol Biochem* 35: 1482–1498, 2015. doi:10.1159/000373967.
87. **Kim JI**, **Park J**, **Ji Y**, **Jo K**, **Han SM**, **Sohn JH**, **Shin KC**, **Han JS**, **Jeon YG**, **Nahmgoong H**, **Han KH**, **Kim J**, **Kim S**, **Choe SS**, **Kim JB.** During adipocyte remodeling, lipid droplet configurations regulate insulin sensitivity through F-actin and G-actin reorganization. *Mol Cell Biol* 39: e00210-19, 2019. doi:10.1128/MCB.00210-19.
88. **Dharuri H**, **'t Hoen PA**, **van Klinken JB**, **Henneman P**, **Laros JF**, **Lips MA**, **El Bouazzaoui F**, **van Ommen GB**, **Janssen I**, **van Ramshorst B**, **van Wagensveld BA**, **Pijl H**, **Willems van Dijk K**, **van Harmelen V.** Downregulation of the acetyl-CoA metabolic network in adipose tissue of obese diabetic individuals and recovery after weight loss. *Diabetologia* 57: 2384–2392, 2014. doi:10.1007/s00125-014-3347-0.
89. **Herman MA**, **She P**, **Peroni OD**, **Lynch CJ**, **Kahn BB.** Adipose tissue branched chain amino acid (BCAA) metabolism modulates circulating BCAA levels. *J Biol Chem* 285: 11348–11356, 2010. doi:10.1074/jbc.M109.075184.
90. **Newgard CB**, **An J**, **Bain JR**, **Muehlbauer MJ**, **Stevens RD**, **Lien LF**, **Haqq AM**, **Shah SH**, **Arlotto M**, **Slentz CA**, **Rochon J**, **Gallup D**, **Ilkayeva O**, **Wenner BR**, **Yancy WS**, **Eisenson H**, **Musante G**, **Surwit RS**, **Millington DS**, **Butler MD**, **Svetkey LP.** A branched-chain amino acid-related metabolic signature that differentiates obese and lean humans and contributes to insulin resistance. *Cell Metab* 9: 311–326, 2009. doi:10.1016/j.cmet.2009.02.002.
91. **Heinonen S**, **Jokinen R**, **Rissanen A**, **Pietiläinen KH.** White adipose tissue mitochondrial metabolism in health and in obesity. *Obes Rev* 21: e12958, 2020. doi:10.1111/obr.12958.
92. **Wiklund P**, **Zhang X**, **Pekkala S**, **Autio R**, **Kong L**, **Yang Y**, **Keinänen-Kiukaanniemi S**, **Alen M**, **Cheng S.** Insulin resistance is associated with altered amino acid metabolism and adipose tissue dysfunction in normoglycemic women. *Sci Rep* 6: 24540, 2016. doi:10.1038/srep24540.
93. **van der Kolk BW**, **Muniandy M**, **Kaminska D**, **Alvarez M**, **Ko A**, **Miao Z**, **Valsesia A**, **Langin D**, **Vaittinen M**, **Pääkkönen M**, **Jokinen R**, **Kaye S**, **Heinonen S**, **Virtanen KA**, **Andersson DP**, **Männistö V**, **Saris WH**, **Astrup A**, **Rydén M**, **Blaak EE**, **Pajukanta P**, **Pihlajamäki J**, **Pietiläinen KH.** Differential mitochondrial gene expression in adipose tissue following weight loss induced by diet or bariatric surgery. *J Clin Endocrinol Metab* 106: 1312–1324, 2021. doi:10.1210/clinem/dgab072.
94. **Jokinen R**, **Rinnankoski-Tuikka R**, **Kaye S**, **Saarinen L**, **Heinonen S**, **Myöhänen M**, **Rappou E**, **Jukarainen S**, **Rissanen A**, **Pessia A**, **Velagapudi V**, **Virtanen KA**, **Pirinen E**, **Pietiläinen KH.** Adipose tissue mitochondrial capacity associates with long-term weight loss success. *Int J Obes (Lond)* 42: 817–825, 2018. doi:10.1038/ijo.2017.299.
95. **Vink RG**, **Roumans NJ**, **Čajlaković M**, **Cleutjens JPM**, **Boekschoten MV**, **Fazelzadeh P**, **Vogel MAA**, **Blaak EE**, **Mariman EC**, **van Baak MA**, **Goossens GH.** Diet-induced weight loss decreases adipose tissue oxygen tension with parallel changes in adipose tissue phenotype and insulin sensitivity in overweight humans. *Int J Obes (Lond)* 41: 722–728, 2017. doi:10.1038/ijo.2017.38.
96. **Perez-Riverol Y**, **Bai J**, **Bandla C**, **García-Seisdedos D**, **Hewapathirana S**, **Kamatchinathan S**, **Kundu DJ**, **Prakash A**, **Frericks-Zipper A**, **Eisenacher M**, **Walzer M**, **Wang S**, **Brazma A**, **Vizcaíno JA.** The PRIDE database resources in 2022: a hub for mass spectrometry-based proteomics evidences. *Nucleic Acids Res* 50: D543–D552, 2022. doi:10.1093/nar/gkab1038.